Inferring the concentration of anthropogenic carbon in the ocean from tracers

Timothy M. Hall
NASA Goddard Institute for Space Studies, New York, New York, USA

Thomas W. N. Haine and Darryn W. Waugh
Earth and Planetary Sciences, Johns Hopkins University, Baltimore, Maryland, USA

Received 19 November 2001; revised 8 February 2002; accepted 14 September 2002; published 14 December 2002.

[1] We present a technique to infer concentrations of anthropogenic carbon in the ocean from observable tracers and illustrate the technique using synthetic data from a simple model. In contrast to several recent studies, the technique makes no assumptions about transport being dominated by bulk advection and does not require separation of the small anthropogenic signal from the large and variable natural carbon cycle. Mixing is included naturally and implicitly by using observable tracers in combination to estimate the distributions of transit times from the surface to interior points. The time-varying signal of anthropogenic carbon in surface waters is propagated directly into the interior by the transit time distributions (TTDs) without having to consider background natural carbon. The TTD technique provides estimates of anthropogenic carbon, as simulated directly in the model, that are more accurate than techniques relying on single tracer "ages" (e.g., CFC age) to represent transport. In general, the TTD technique works best when at least two tracers are used in combination, and the tracers have significantly different timescales in either their surface temporal variation or radioactive decay. Possibilities are a CFC or CCl_4 in combination with natural $\Delta^{14}C$ or ^{39}Ar. However, even for a CFC alone the TTD technique results in less bias for anthropogenic carbon estimates than use of a CFC age. *INDEX TERMS:* 1615 Global Change: Biogeochemical processes (4805); 1635 Global Change: Oceans (4203); 4568 Oceanography: Physical: Turbulence, diffusion, and mixing processes; 4806 Oceanography: Biological and Chemical: Carbon cycling; 4808 Oceanography: Biological and Chemical: Chemical tracers; *KEYWORDS:* carbon cycle, ocean carbon uptake, ocean tracers, ocean transport, transit-time distribution

Citation: Hall, T. M., T. W. N. Haine, and D. W. Waugh, Inferring the concentration of anthropogenic carbon in the ocean from tracers, *Global Biogeochem. Cycles*, *16*(4), 1131, doi:10.1029/2001GB001835, 2002.

1. Introduction

[2] The ocean is a major buffer to the increasing levels of atmospheric CO_2 caused by anthropogenic emissions. According to the Intergovernmental Panel on Climate Control (IPCC), best estimates indicate that roughly one third of the carbon from these emissions is sequestered by the ocean. However, there remains great uncertainty in the rate of uptake and the amount of anthropogenic carbon that presently resides in the ocean. Better quantification of the ocean's role in the perturbed carbon cycle is one of the major challenges for carbon cycle science [*Sarmiento and Wofsy*, 2000].

[3] There has been considerable effort to estimate the ocean inventory of anthropogenic carbon from measurements of total carbon [see *Wallace*, 2001, and references therein]. A major difficulty is separating the small anthropogenic signal (order 1%) from the much larger natural signal, which is variable due to biogeochemical sources and sinks. *Gruber et al.* [1996] have developed one of the most detailed techniques to perform such separation, and application of the method has resulted in estimates of anthropogenic carbon inventories accumulated since preindustrial times in several ocean regions [*Gruber*, 1998; *Sabine et al.*, 1999]. These analyses represent an important contribution to the interpretation of ocean carbon measurements, but there are several sources of uncertainty and possible bias. For example, to separate ΔDIC (the anthropogenic component of total dissolved inorganic carbon) from the DIC due to remineralization of organic material a stoichiometric carbon to oxygen ratio R is assumed (Redfield ratio). *Wanninkhof et al.* [1999] have shown that realistic uncertainty in R can lead to large fractional errors at moderate levels of ΔDIC (e.g., 30% to 50% error for ΔDIC of 30 μmole/kg).

[4] Additionally, the approaches of *Gruber et al.* [1996] and others [e.g., *Thomas and Ittekkot*, 2001] rely on knowl-

0886-6236/02/2001GB001835$12.00

edge of "age," construed as the time since the water under analysis last made surface contact. Ages derived from chlorofluorocarbons (CFCs) and tritium helium combinations ($^3H/^3He$) have commonly been used. Recently, *Wallace* [2001] has pointed out the need for an improved approach for water masses having negligible CFCs but significant ΔDIC, which is expected because anthropogenic CO_2 has been present in the atmosphere much longer than CFCs (250 years compared to 50 years). More fundamentally, the age approach suffers from a basic flaw: It rests on the assumption that a water mass has a single transit time since last surface contact, equivalent to an assumption of pure bulk advection. While the impact of mixing on tracer ages has been a subject of considerable study [e.g., *Thiele and Sarmiento*, 1990], recent theoretical work has made explicit the fact that in any flow involving mixing there is a continuous distribution of transit times from one region to another [*Beining and Roether*, 1996; *Khatiwala et al.*, 2001; *Deleersnijder et al.*, 2001; *Haine and Hall*, 2002]. No single age, whether a CFC age or otherwise, can completely summarize the transport.

[5] It is the transit time distribution (also called the "age spectrum"), rather than any single age, that is a fundamental descriptor of the transport from one region to another. The transit time distribution (TTD) implicitly includes the effects of bulk advection and mixing. Indeed, the integrated effects of all transport mechanisms are included, although none need be represented explicitly. If the TTDs from all surface source regions were fully known in the ocean, then the distribution and evolution of any passive and conservative constituent could be determined solely from knowledge of the constituent's space and time variation in surface waters [*Haine and Hall*, 2002]. Alternatively, if the TTD from the outcrops of an isopycnal surface were known, then the distribution and evolution of a passive and conservative constituent on the surface could be determined solely from knowledge of its variation at the outcrops, to the extent that diapycnal mixing is negligible. Finally, if a constituent is approximately uniform over the ocean surface, varying only in time, then that time variation and the TTD from the full surface would be sufficient to determine interior concentrations of the tracer. This last approach is taken by *Thomas et al.* [2001], who used model-generated TTDs from the full surface to determine anthropogenic carbon inventories from a reconstruction of ΔDIC in surface waters. Their analysis, however, is subject to the error of the model transport.

[6] Here we explore the possibility of extending the *Thomas et al.* [2001] approach by using TTDs derived from combinations of observable tracers, rather than from models, to estimate ΔDIC. Because all tracer signals are propagated from the surface to the interior by TTDs, observations of these tracers provide information on TTDs. If sufficient information can be gleaned, TTDs can be estimated and used to propagate anthropogenic carbon, given knowledge of its surface time variation. This technique does not depend on model transport, and because direct measurements of DIC are not required, it avoids the inherent uncertainties of the separation of anthropogenic and natural carbon. It is important to note that most ΔDIC inference techniques, including the TTD technique, share common assumptions. Anthropogenic carbon is assumed to be a linear perturbation to the ocean carbon cycle (that is, rising carbon levels have not caused significant changes in biogeochemical cycles), and neither the spatial distribution of surface air-sea fluxes nor the ocean circulation itself have changed significantly since preindustrial times. The TTD technique has the benefit of relaxing an additional and highly questionable assumption made in many previous studies; namely, that ocean transport is purely bulk advective.

[7] This paper constitutes a "test-of-concept" study using a simple model as a laboratory ocean. In subsequent work we plan to use more sophisticated models to explore the limits of the approximations made and to apply the technique to tracer measurements. The paper is organized as follows: In section 2 we review briefly the theory of the TTD. In section 3 we describe the simple model that serves as our laboratory ocean. Section 4 introduces the tracers to be used, and section 5 contains our analysis. In section 6 we make some comparisons to the approach of *Gruber et al.* [1996]. We summarize in section 7.

2. Transit Time Distribution

[8] Our analysis exploits the conceptual framework of the "transit time distribution," (TTD) variously known as the age spectrum, the age distribution, the transit-time probability density function, the boundary propagator, and the Green's function for boundary conditions. The TTD and related quantities have a long history in a variety of disciplines (see the review by *Waugh and Hall* [2002]). In an atmospheric context, it has been developed formally by *Hall and Plumb* [1994] and *Holzer and Hall* [2000]. In an ocean context the TTD and related quantities have been discussed in several studies [*Beining and Roether*, 1996; *Delhez et al.*, 1999; *Khatiwala et al.*, 2001; *Deleersnijder et al.*, 2001; *Haine and Hall*, 2002]. We review the TTD only briefly here.

[9] The TTD, $\mathcal{G}(r, \xi)$, is the distribution of transit times ξ since a water parcel at point r last had contact with a specified surface region S (which could be the full ocean surface); that is, the quantity $\mathcal{G}(r, \xi)\, d\xi$ is the mass fraction of the parcel that made last contact with S a time ξ to $\xi + d\xi$ ago. The TTD for pure bulk advection from S to r at rate u is $\delta(\xi \quad |r|/u)$, where $\delta(\xi)$ is the Dirac delta function. Generally, however, a broad distribution of transit time exists, due in part to the fact that various subregions of S having different proximities to r contribute to the water at r. Even if S represents a single surface source region, however, there is a wide distribution of times, because shear flows and eddies cause transport pathways to diverge and become convoluted. *Haine and Hall* [2001] have extended the TTD framework to encompass distributions with respect to surface sources regions (i.e., components of S), thereby including the classical concept of water mass composition by surface region. Here, however, we restrict attention to a single surface region, which is assumed to have uniform (but time varying) tracer concentrations.

[10] The TTD is a type of Green's function that propagates a boundary condition (BC) on tracer mole fraction in surface waters into the interior. For a tracer of mole fraction

q with a known surface layer time history $q(r_S, t)$ interior values can be written

$$q(r,t) = \int_0^\infty q(r_S, t \quad \xi)\mathcal{G}(r,\xi)\, d\xi \qquad (1)$$

(assuming stationary transport and uniform q over the surface region). For a tracer that is decaying radioactively or undergoing uniform chemical loss at rate λ, a similar expression holds, but with an additional factor $e^{\quad \lambda\xi}$ in the integral. The TTD is always positive, and $\int_0^\infty \mathcal{G} d\xi = 1$ everywhere (for a finite domain with nonzero diffusion), which is simply the statement that all the water in a parcel must have at some past time made surface contact. Without any knowledge of the circulation, there is little additional restriction on $\mathcal{G}$. The task is to deconvolve expression (1) from measurements of q to obtain information on $\mathcal{G}$ that can be applied to ΔDIC.

[11] While it is possible to approach the deconvolution without any assumptions on the form of $\mathcal{G}$ [e.g., *Johnson et al.*, 1999], we use a parametric technique based on our expectation that $\mathcal{G}$ often has a relatively simple shape. In the numerical ocean studies of *Khatiwala et al.* [2001], *Haine and Hall* [2002] and *Thomas et al.* [2001] the TTD are broad and asymmetric, with an early peak and long tail. Other advective-diffusive systems display similar TTD shapes, for example numerical models of the stratosphere [e.g., *Hall et al.*, 1999]. The TTDs may have this shape because direct pathways from the surface to interior points dominate the transport, causing short transit times to be the most common, while along-flow and lateral mixing result in the additional presence of widely varied longer transit times. Whatever the reason, the relative simplicity of shape suggests that only a few parameters can go a long way to characterize the TTD. Therefore, we write the TTD with a simple functional form having this shape and estimate the free parameters of the function from tracer observations.

[12] The functional form we employ, sometimes called an "inverse Gaussian" (IG) distribution [*Seshadri*, 1999], is a solution to the one-dimensional advection-diffusion equation. However, we make no dynamical arguments for the relevance of one-dimensional transport, and the solution is merely a convenient form whose parameters are varied freely at each location to best match the tracer observations. In terms of the "mean transit time" Γ (the first temporal moment of $\mathcal{G}$, also referred to as the "mean age") and a measure Δ of the spread of transit times (the centered second temporal moment)

$$\mathcal{G}(t) = \frac{1}{2\Delta\sqrt{\pi t^3}} \exp\left(\frac{\Gamma^2(t \quad 1)^2}{4\Delta^2 t}\right) \qquad (2)$$

where $t = \xi/\Gamma$ is a dimensionless time [*Waugh and Hall*, 2002].

[13] The simple IG form cannot fully represent the complexity of real ocean transport, nor even fully the transport in simple ocean models (see below). It would be possible, of course, to describe the TTD with more flexible functional forms having additional free parameters; this would necessitate additional observational constraints. We note, however, that in previous observational analyses of anthropogenic carbon a single age has been used to represent transport, equivalent to assuming a delta function for the TTD. (Note that $\lim_{\Delta\to 0}\mathcal{G}(t) = \delta(t \quad \Gamma)$ in (2) above.) By permitting nonzero Δ our approach constitutes, in effect, a next level of approximation of the TTD.

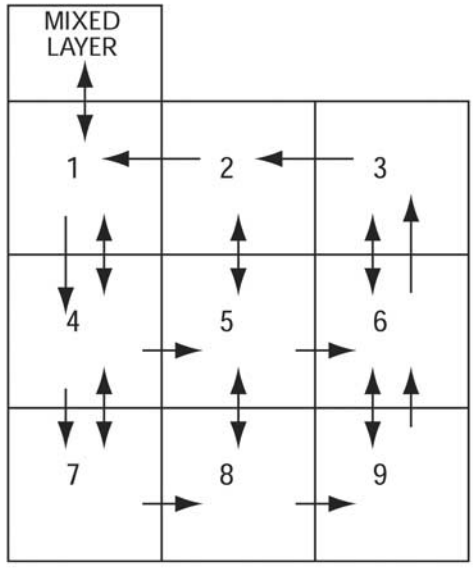

Figure 1. Schematic of nine-box model. One-sided arrows indicate advective fluxes. Two-sided arrows indicate diffusive fluxes. Arrow lengths are proportional to flux magnitudes.

3. Model

[14] To illustrate the TTD approach to ΔDIC estimation, we employ the nine box model described by *Haine and Hall* [2002], and summarized schematically in Figure 1. The model has diffusive and advective fluxes coupling the interior boxes. The upper left box is coupled diffusively to a mixed layer on which time-dependent boundary conditions (BCs) on tracer mole fraction are applied.

[15] Physically, the model may be thought of as representing a hemispheric meridional overturning cell whose penetration of tracer from the mixed layer to the interior is restricted to high latitudes. Alternatively, it can be considered a circulation on an isopycnal surface with the mixed layer exchange representing a single outcrop. No attempt has been made to "tune" the model to any particular ocean circulation, and we do not defend its realism in detail. Our goal is to generate examples of TTDs that are similar to those of more sophisticated numerical models. Our guide in selecting the magnitude of fluxes is to have significant amounts of ΔDIC throughout the domain, thereby allowing the best comparison to the analysis on the "fully contaminated" isopycnal surfaces of *Gruber et al.* [1996]. In section 5.4 we examine sensitivity to the circulation.

[16] The TTD for the nine box model, shown in Figure 2, can be computed from an eigenvalue analysis or as the time-dependent response to a $\delta(t)$ BC on the mixed layer [*Haine and Hall*, 2002]. The model captures important features of TTDs seen in ocean GCM studies [*Khatiwala et al.*, 2001;

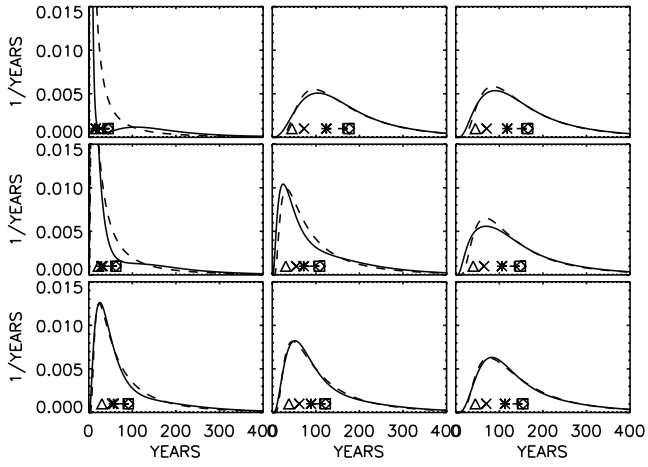

Figure 2. TTD for the box model (solid line) and the best-fit two-parameter TTD (dashed line). Panels corresponds to model boxes, as displayed in Figure 1. Also shown as symbols are τ_{CFC} (triangle), τ_{CCl4} (cross) τ_{DIC} (asterisk), τ_{39Ar} (plus), τ_{14C} (square), and Γ (diamond).

Thomas et al., 2001; *Haine and Hall*, 2002]. The TTD are broadly distributed with early peaks and long tails. With increasing distance from the mixed layer along the dominant advective pathway, the TTDs broaden and shift to longer transit times. The TTD of box 1, which receives direct input from the mixed layer, is bimodal, reflecting the early peak of the adjacent source water, and the secondary broad, low peak due to recirculated waters from below. (Similar weak bimodality was seen in the North Atlantic gyre of the *Haine and Hall* [2002] numerical study.) While the nine box model TTDs do not have high frequency structure, such structure is largely irrelevant to this study, since the tracer fields represent integrations over many decades of transit time (see section 5.4). For the sake of this test-of-concept analysis, we take the nine box TTD and its tracer fields, including ΔDIC, as "truth." The tracer fields are considered "observations" to be used to estimate ΔDIC, and the estimates are compared to the "true" ΔDIC.

4. Tracers and Tracer Ages

[17] In our analysis we use the tracers CFC11, CCl_4, natural $\Delta^{14}C$, ^{39}Ar, and ΔDIC. For the transient tracers (CFC11, CCl_4, ΔDIC) a time-dependent BC is applied on the model's mixed layer and the interior response is calculated. For the radioisotopes (^{39}Ar, $\Delta^{14}C$) the BC is constant, and radioactive decay applies in the interior with the e-folding times of 390 years for ^{39}Ar and 8270 years for $\Delta^{14}C$. Although not exhaustive, the tracers we select cover a wide range of timescales. Other observable tracers are available, particularly CFC12, bomb-radiocarbon and bomb-^3H and ^3He. CFC12 has a surface history very similar to CFC11, and would work as well as CFC11 in our analysis. But once either CFC11 or CFC12 is selected the other tracer provides little additional constraint on ΔDIC. In our simple model $^3H/^3He$ in combination with CFC11 provides only marginal improvement in ΔDIC estimation over CFC11 alone. However, *Waugh et al.* [2002], who discuss relationships among tracer ages in more detail (including CFCs, CCl_4, $^3H/^3He$ and their ability to constrain age spectra) find circumstances in which $^3H/^3He$ and a CFC are useful in combination.

4.1. CFC11 and CCl_4

[18] A number of studies in recent years have made use of CFCs (CFC11, CFC12, CFC113) and CCl_4 as tracers to estimate pathways and rates of ocean circulation and to evaluate general circulation models [e.g., *Wallace et al.*, 1994; *Haine et al.*, 1998; *England and Maier-Reimer*, 2001]. CFC11 and CFC12 are passive and inert in seawater and have no interior sources. There is evidence for temperature-dependent chemical loss of CCl_4 [*Meredith et al.*, 1996; *Huhn et al.*, 2001], which we include in a simple fashion here (see below). Until the 1990s, the concentrations of CFCs and CCl_4 had increased steadily in the atmosphere since the beginning of industrial sources in the 1940s for CFCs and 1920s for CCl_4. The atmospheric signals have penetrated the ocean. Plotted in Figure 3 are the boundary layer time series used in the model for CFC11 and CCl_4. These series were converted from the atmospheric histories of *Walker et al.* [2000] using published solubility factors [*Hunter-Smith et al.*, 1983; *Warner and Weiss*, 1985] for $T = 6$ C and $S = 35$pss (typical of water in the North Atlantic subpolar gyre) and assuming 100% saturation. Other choices for solubility (T, S) and surface

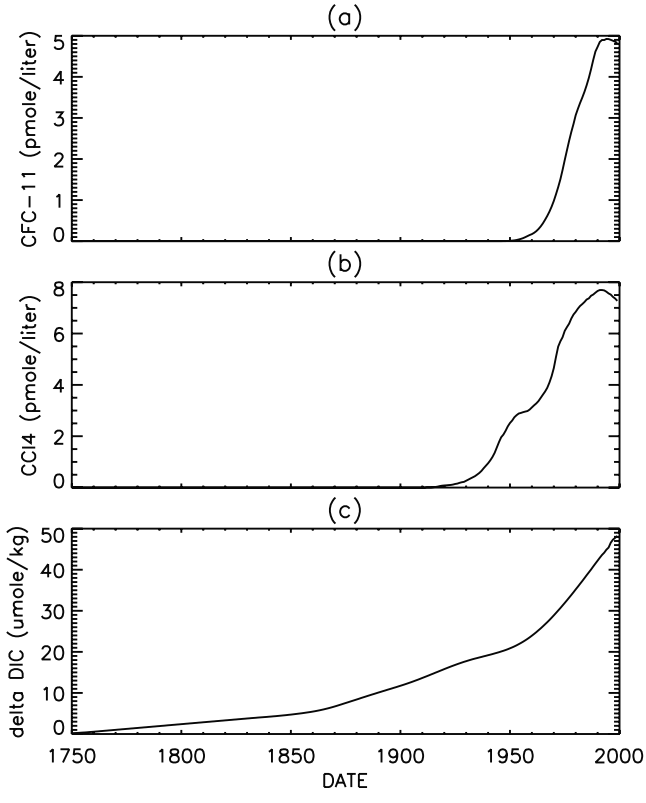

Figure 3. Surface layer time-dependent boundary conditions for (a) CFC11, (b) CCl4, and (c) ΔDIC.

saturation would serve equally well in this test-of-concept analysis.

[19] Our analysis requires a figure for the uncertainty of the tracers as constraints on transport. Sources of this uncertainty are measurement error, uncertainty in the BC in surface waters, and, for CCl_4, chemical loss. The boundary uncertainty is comprised of uncertainty in the solubility, saturation, and atmospheric history. Based on these considerations, *Doney et al.* [1997] estimate uncertainties for CFCs in terms of their ages (the lag times of a CFC at interior ocean points from the surface layer evolution) of ±0.5 years for present day values, increasing to ±5 years for values before 1950. We convert the ages to mole fractions to obtain an effective uncertainty for CFC11. The 5-year uncertainty is based in part on an assumed 10% uncertainty in the early atmospheric CFC abundance, which is larger than the uncertainty in abundance estimated by *Walker et al.* [2000]. We have chosen to use the larger uncertainty of ±0.5 to ±5.0 years, because it encompasses better the error in assuming 100% saturation, and in general provides a more conservative assessment of the TTD technique.

[20] We have less guidance for CCl_4. The CCl_4 solubility factor is thought to be less well established than for CFCs [e.g., *Wallace et al.*, 1994], and the atmospheric history has greater uncertainty [*Walker et al.*, 2000]. In addition the nature and rate of chemical loss of CCl_4 is uncertain. For T = 6 C used in these model experiments *Huhn et al.* [2001] estimate a loss rate of about 1.5%/year (see their Figure 13), with a range from 0.0% (conservative) to about 3%/year. Thus, in our simulations of CCl_4 we apply a uniform 1.5%/year loss, while in the subsequent TTD analysis we try a range of loss rates from 0.0 to 3%/year to mimic realistic uncertainty. At each assumed loss rate, we use the CFC age uncertainty increased uniformly by 50% (to account for higher uncertainty in solubility and atmospheric history) and converted to CCl_4 mole fractions. The total uncertainty is the union of the uncertainties for each assumed loss rate. The loss rate increases rapidly with temperature. A similar analysis in colder waters would incur less uncertainty, while the loss in much warmer waters (up to 25%/year above 14 C) would negate the tracer utility of CCl_4.

4.2. ^{39}Ar and Δ^{14}C

[21] Many studies have exploited the radioisotope ^{14}C to diagnose transport [e.g., *Broecker et al.*, 1988], and several have analyzed the sparse measurements of ^{39}Ar [e.g., *Schlitzer et al.*, 1985]. These radioisotopes have atmospheric sources and, upon entering the ocean by gas exchange, decay with e-folding times of 390 years for ^{39}Ar and 8270 years for ^{14}C. There are advantages to considering the ratio $\Delta^{14}C = {}^{14}C/{}^{12}C$, instead of ^{14}C alone. The two carbon isotopes undergo similar biochemical transformations, so that to a good approximation the ratio acts as a radioactive tracer with no interior chemical sources or sinks [*Fiadiero*, 1982]. We adopt this approach here.

[22] ^{39}Ar is an attractive tracer. Its concentration in surface waters equilibrates rapidly enough with the atmosphere that the surface saturation is near 100%. Its 390-year timescale is complementary to the shorter timescales of CFCs and the longer timescale of Δ^{14}C. In addition, the dominant source of ^{39}Ar, natural upper atmospheric cosmogenesis, is steady. Unfortunately, the extremely small isotopic abundance of ^{39}Ar makes its measurement challenging and expensive. Thus, effective uncertainty in ^{39}Ar is dominated by the measurement uncertainty, which is significant because large sample volumes and long decay counts are required. We choose an uncertainty of ±5%, corresponding roughly to ^{39}Ar uncertainties quoted by *Broecker and Peng* [2000]. The inclusion of ^{39}Ar in this study might reasonably be questioned, given the paucity of measurements and the fact that the TTD method has merit independent of the use of ^{39}Ar as a constraint. We include it in part to explore the extent to which ^{39}Ar data could be useful for ΔDIC estimation if less expensive measurement techniques were developed. Additionally, the few present data may provide a useful check on TTD estimates from other tracers.

[23] Δ^{14}C equilibrates with the atmosphere much more slowly, resulting in surface water depletions of Δ^{14}C by more than 4%, equivalent to Δ^{14}C ages of more than 300 years. Moreover, in addition to the steady cosmogenic source, present day Δ^{14}C is a response to the small source from fossil CO_2 via the Suess effect, and, importantly, the large input from the 1960s atmospheric bomb tests. We are interested here in the long timescale of the decay of natural Δ^{14}C. (In our simple model, bomb Δ^{14}C in combination with CFC11 offers only marginal gain in ΔDIC estimation over CFC11 alone.) Thus, the effective uncertainty on natural Δ^{14}C is largely set by the ability to separate natural and bomb radiocarbon at the surface (for the BC) and in the interior. *Broecker et al.* [1995] show latitudinal profiles of bomb Δ^{14}C separated from natural Δ^{14}C along various isopycnal surfaces with a scatter of ±10 to ±20 permil, corresponding to an equivalent uncertainty in the remaining natural Δ^{14}C; i.e., ±1 to ±2%. This turns out to be near the threshold of what is useful in our study of ΔDIC estimation. We employ the figure ±1%, keeping in mind that doubling the uncertainty would result in Δ^{14}C that is a less useful constraint. Of course, even with larger uncertainty, deep depletion of Δ^{14}C (e.g., Δ^{14}C ages of 500 to 1000 years in the deep tropical Pacific [*Broecker and Peng*, 2000]) represents an important constraint, by indicating negligible levels of ΔDIC.

4.3. ΔDIC

[24] DIC in the equilibrium marine carbonate system can be determined from the partial pressure of atmospheric CO_2 (pCO_2), total alkalinity, temperature (T) and salinity (S). We take the basic approach of *Thomas et al.* [2001] and *Thomas and Ittekkot* [2001] and use the "CO2sys" program [*Lewis and Wallace*, 1998] (available at http://cdiac.esd.ornl.gov/oceans/co2rprt.html) to solve for DIC, given T and S typical of the North Atlantic subpolar gyre (T = 6 C and S = 35pss) and pCO_2 from 1750 to the present day (pCO_2 data at http://www.giss.nasa.gov/data/si2000/ghgases). Alkalinity is set to 2300 μmole/kg, also typical of the North Atlantic [*Millero et al.*, 1998]. From each value of DIC we subtract the value for the year 1750, thus providing a time series of ΔDIC. This serves as our time

dependent BC. Note that compared to *Thomas et al.* [2001] no linearization of ΔDIC in T and S is required or performed.

[25] The *Thomas et al.* [2001] approach of propagating a ΔDIC BC has the advantage that anthropogenic carbon, rather than total carbon, is considered from inception, so that no separation of the small anthropogenic signal from the large and variable natural signal is required. Furthermore, when one makes the approximation, as has been done in most other methods, that the disequilibrium across the air-sea interface has changed little since preindustrial times, then the *Thomas et al.* [2001] method also has the advantage of not requiring any knowledge of that disequilibrium. The disequilibrium term vanishes upon forming the difference $\Delta DIC = DIC(t) \quad DIC_{pre}$, where DIC_{pre} is the preindustrial level.

[26] There are several sources of uncertainty in the BC for ΔDIC that, in principle, impact the inference of interior ΔDIC concentrations. Among these is the lack of a universally agreed upon best set of dissociation coefficients for the equilibrium carbonate system. A full exploration of the sensitivity of inferred ΔDIC to this and other uncertainties in the BC is beyond the scope of this study, although such an exploration should be performed before applying the age spectral technique to observations. However, two points can be made here: (1) The impact of these uncertainties on ΔDIC will be significantly smaller than the impact on DIC. For example, we use the carbonate dissociation coefficients of *Roy et al.* [1993]. A preliminary investigation using CO2sys suggests that the impact on ΔDIC (as opposed to DIC) of using the dissociation constants of *Goyet and Poissonn* [1989] or *Mehrbach et al.* [1973], as refit by *Dickson and Millero* [1987], is only about 1 μmole/kg. (2) Uncertainties in the ΔDIC BC also affect most other ΔDIC inference techniques, including *Gruber et al.* [1996] (see Section 6). Thus, for the purpose here of testing relative advantages of the TTD technique, the sensitivity to uncertainty in the ΔDIC BC is not included.

[27] Finally, we emphasize that the "true" ΔDIC (that simulated directly in the model) is a strictly passive and conservative tracer. Carbon chemistry largely determines the ΔDIC concentration in surface waters, but we assume the results of this process to be known, thus establishing the BC. No subsequent biochemical transformations are included. We are in effect testing the ability to infer one tracer with a known time-dependent BC from other tracers with different known time-dependent BCs. ΔDIC in the real ocean is a passive and conservative tracer only to the extent that increasing DIC levels have not caused changes in rates of biochemical processes in the interior ocean. Modeling evidence suggests this is a reasonable approximation [*Maier-Reimer et al.*, 1996; *Plattner et al.*, 2001], although it warrants further study. It is also the same approximation made in other ΔDIC inference techniques, including *Gruber et al.* [1996].

4.4. Tracer Ages

[28] Transient tracer ages, sometimes called concentration or partial pressure ages, have been exploited extensively to diagnose transport [e.g., *Doney et al.*, 1997]. They are defined as the lag times of the tracer evolution at interior points with respect to the surface layer. Radioactive tracer ages have also been used extensively for this purpose [e.g., *Jenkins*, 1987; *Broecker et al.*, 1988], and are defined as $\lambda^{-1} \ln(q_{obs}/q(0))$, where λ is the relevant radioactive e-folding decay rate, q_{obs} the observed isotopic abundance and $q(0)$ the abundance at the surface.

[29] To illustrate the behavior of these tracer ages, we plot as symbols in Figure 2 tracer ages obtained from CFC11, CCl_4, ΔDIC (assuming it were known), $\Delta^{14}C$, and ^{39}Ar, as well as the mean transit time. These are denoted τ_{CFC}, τ_{CCl4}, τ_{DIC}, τ_{14C}, τ_{39Ar} and Γ, respectively. The ages all strictly differ from one another, with $\tau_{CFC} < \tau_{CCl4} < \tau_{DIC} < \tau_{39Ar} < \tau_{14C} < \Gamma$. (Note that all the ages are equal for pure bulk advection.) In general, the tracer with the shortest history or most rapid radioactive decay will weight most heavily the early components of the TTD, resulting in the smallest tracer age [*Waugh et al.*, 2002]. CFC11 is only sensitive to the first 50 years of the spectrum and CCl_4 to the first 80 years (the times they have been present in the atmosphere), resulting in smaller timescales. The radioisotopes have longer timescales, while Δ*DIC* is intermediate. Note that *Coatanoan et al.* [2001], as part of a comparison of carbon inventory techniques, observe that τ_{DIC} (using the ΔDIC obtained from the "MIX" technique of *Goyet et al.* [1999]) is larger than τ_{CFC} and speculate as to the cause. Part of the difference they observe is a fundamental consequence of tracers having different time-dependent surface variations in the presence of a wide TTD.

[30] For the age spectra of Figure 2, τ_{14C} and Γ are indistinguishable. When a tracer's time variation, either because of transience or radioactive decay, is roughly linear over the width of the TTD its age approximates the mean transit time [*Hall and Plumb*, 1994]. Compared to these age spectra, $\Delta^{14}C$ decays very slowly, and therefore approximately linearly, and so $\tau_{14C} \quad \Gamma$. This is true for ^{39}Ar only to a lesser degree, and τ_{39Ar} can be distinguished from Γ for most of the age spectra in Figure 2.

5. Analysis

[31] Our procedure to test the use of the TTD in estimating ΔDIC proceeds as follows: We use the model to simulate the TTD, CFC11, CCl_4, natural $\Delta^{14}C$, ^{39}Ar, and ΔDIC. Our goal is to estimate ΔDIC using the tracer "observations," that is values of CFC11, CCl_4, $\Delta^{14}C$, and ^{39}Ar simulated directly by the model. We check first how accurately the IG TTD estimates ΔDIC, given perfect knowledge of the mean transit time Γ and spectral Δ from the true age spectra (i.e., the model generated age spectra). We then use various tracers observations singly and in combination, allowing for measurement uncertainty, to estimate Γ and Δ. These estimates of Γ and Δ provide a range of IG age spectra, which in turn are used to construct estimates of ΔDIC. The estimated ΔDIC are then compared to the true values (the values simulated directly by the model) to evaluate the procedure.

[32] It is possible to bypass the TTD completely in this analysis. Because ΔDIC is estimated as a function of Γ and Δ, and Γ and Δ are estimated from tracers, we could express ΔDIC directly as a function of tracer concentra-

tions. We prefer to maintain the TTD as an intermediate step for two reasons: (1) The TTD has a physical interpretation; (2) The TTD approach is more general, because other constituents in addition to ΔDIC could, in principle, be estimated.

5.1. Impact of Assumed TTD Functional Form

[33] In addition to the true (model) TTD, the IG TTD, with Γ and Δ set equal to the values of the true TTDs, are plotted superposed in Figure 2 as dashed lines. These are the "best-fit" IG TTD. The IG functional form does not permit bimodality, and so the comparison to the true TTDs is poorest in boxes 1 and 4. In other boxes the IG TTDs mimic the true TTDs more closely.

[34] The best-fit IG age spectra are used to construct ΔDIC by convolution with the ΔDIC BC, according to expression (1). In Figure 4 these ΔDIC values are plotted as diamonds for each model box. Also plotted for comparison is ΔDIC inferred by lagging the ΔDIC surface history by τ_{CFC}, the approach taken by *Thomas and Ittekkot* [2001]; ΔDIC inferred by using Γ as a lag; and ΔDIC employing the transport component of the *Gruber et al.* [1996] technique, which uses τ_{CFC} in a more restrictive fashion (see section 6). The true ΔDIC concentrations are indicated in Figure 4 by the horizontal lines. In all boxes (except box 1) the best-fit IG TTD ΔDIC is the best estimate of the "true" ΔDIC. The τ_{CFC}-lagged ΔDIC is everywhere an overestimate. The value of τ_{CFC} is only sensitive to components of the TTD less then 50 years, whereas much ΔDIC has older surface origins (see Figure 3). In contrast, the Γ-lagged ΔDIC is everywhere an underestimate: Γ is strongly influenced by very long transit times, which correspond to water with little or no ΔDIC, since significant anthropogenic CO_2 was not present in the atmosphere before 1750. (It is possible, for example, in a slower circulation to have Γ > 250 years, thereby predicting ΔDIC = 0 according to the Γ-lag method, even though there are still significant water components at younger ages having nonzero ΔDIC.)

[35] The only single age that could be used to infer ΔDIC accurately by lagging the surface ΔDIC history is the age of a hypothetical tracer whose surface BC was similar to that of ΔDIC. (A hypothetical radioactive tracer with constant atmospheric abundance and decaying in the ocean with an e-folding time of 40 years, roughly matching the approximate exponential growth in anthropogenic CO_2, would also work.) No such tracer is known. Instead, we aim to use observable tracers in combination to estimate the age spectrum, a more complete transport descriptor than any single age, and use the TTD to estimate ΔDIC.

5.2. TTD Moments From Tracers

[36] The results shown in Figure 4 suggest that knowledge of just two moments of the TTD could help improve ΔDIC inferences. Unfortunately, in reality we do not know Γ and Δ for water masses. Can Γ and Δ be determined from observable tracers with sufficient accuracy to allow useful ΔDIC estimates? This is the question we address next.

[37] We aim to find the (Γ, Δ) pairs that result in a match to the observations. We sweep through ranges of Γ and Δ,

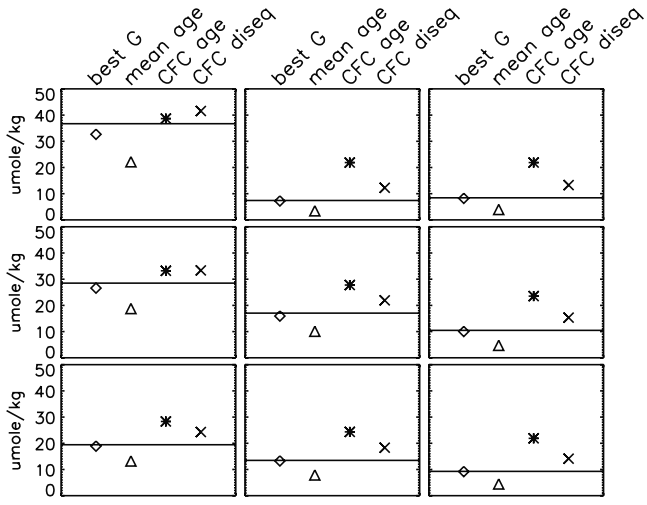

Figure 4. Δ*DIC* for each model box as estimated by the best-fit two-parameter spectra (diamond); lagging by Γ (triangle); lagging by τ_{CFC} (asterisk); and by employing the transport component of the *Gruber et al.* [1996] technique (cross), which uses τ_{CFC} in a more restrictive fashion (called "CFC diseq" above; see text). The true Δ*DIC* (computed directly by the model) is indicated by the horizontal line.

constructing an IG TTD for each (Γ, Δ) pair. These TTD are used to estimate concentrations for CFC11, CCl_4, $\Delta^{14}C$, and ^{39}Ar by convolution with the tracers' BCs and radioactive decay. We then record the range of (Γ, Δ) that match each tracer observation (i.e., model simulated concentrations) within a tolerance equal to the tracer's uncertainty. Figure 5 shows examples of this procedure. Contours of CFC11, CCl_4, $\Delta^{14}C$, and ^{39}Ar constructed from the IG TTD as functions of Γ and Δ are repeated for model boxes 1, 5, and 9. The loci of (Γ, Δ) that result in the "observed" concentrations are plotted as dashed lines; these lines are surrounded by shaded regions representing the tracer uncertainty.

[38] No single tracer can fix both Γ and Δ simultaneously, even given zero uncertainty. Instead, for each tracer there is a locus of (Γ, Δ) points that result in a match to the true value, generally sweeping up to the right from small to large Γ and Δ. To understand the shape of the locus, consider first CFC11. The smallest (Γ, Δ) pair intersects the x-axis, corresponding to a delta function TTD (zero width) peaked at $\Gamma = \tau_{CFC}$. These purely advective age spectra are not ruled out by CFC11 alone. However, higher Γ are also not ruled out, if the corresponding TTD are wider (increasing Δ). Now, IG TTD become increasingly asymmetric with increasing Δ. Therefore, these larger (Γ, Δ) values represent the possibility that the water mass under consideration has young components (early TTD peaks) containing high concentrations of CFC11 mixed with old components (long TTD tails) containing little or no CFC11, such that the observed CFC11 is matched. Water in box 9 is old enough that the observed CFC11 value is not different than zero within the uncertainty, and so the allowed (Γ, Δ) range covers much of the lower right half of the parameter space. This

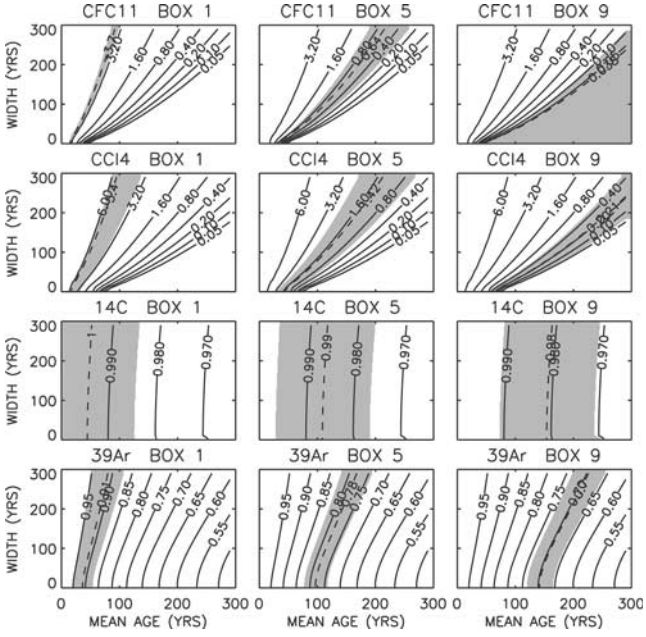

Figure 5. Contour plots of concentration as functions of mean transit time (Γ) and width (Δ) at model boxes 1, 5, and 9 of CFC11 (top row), CCl_4 (second row), $\Delta^{14}C$ (third row), and ^{39}Ar (bottom row). The observed value of the tracer (the value simulated directly by the model) is represented by the dashed contour. Shaded regions indicate the (Γ, Δ) ranges that result in a match to the observed value, within an assumed observational uncertainty (see text). Contour units are pmole/kg for CFC11 and CCl_4 and dimensionless fraction of surface water values for $\Delta^{14}C$ and ^{39}Ar.

absence of CFC11, however, still constitutes a constraint: All (Γ, Δ) that result in nonzero CFC11 are ruled out.

[39] Due to its longer atmospheric history, CCl_4 concentrations are significantly nonzero throughout the domain. The CCl_4 contours are almost parallel to those of CFC11 for large Γ and Δ. For small Δ, however, they differ, with CCl_4 hitting the $\Delta = 0$ axis at larger Γ. Thus, taken in combination, CFC11 and CCl_4 rule out small values of Γ and Δ, but provide no upper bound on Γ or Δ. Large Γ and Δ correspond to the presence of very old components of water, which contain no CFC11 or CCl_4. Therefore, CFC11 or CCl_4 provide no information about these old components, and cannot put upper bounds on Γ and Δ.

[40] The $\Delta^{14}C$ contours are nearly vertically oriented. Because $\Delta^{14}C$ decay is very slow for the timescales of this circulation, and therefore nearly linear over the age spectra, τ_{14C} Γ, approximately independent of Δ. That the $\Delta^{14}C$ contours are oriented differently than those of CFC11 and CCl_4 means that $\Delta^{14}C$ is an independent constraint, so that in combination with CFC11 or CCl_4 a single solution for (Γ, Δ) can be calculated, in principle. The limiting factor is that $\Delta^{14}C$ decays little over the timescales of this circulation, so that the measurement uncertainty represents a large fraction of the ranges in Γ and Δ. For ^{39}Ar the situation is intermediate between CFC11 (or CCl_4) and $\Delta^{14}C$, reflecting the fact that the ^{39}Ar radioactive e-folding time of 390 years is intermediate between the 50 to 80 year history of the transient tracers and the 8270 year e-folding time of $\Delta^{14}C$.

[41] Figure 6 shows examples of the tracer constraints used in combination on model box 9. For CFC11 and $\Delta^{14}C$ the matching lines intersect at (Γ, Δ) (160yrs, 80yrs). However, the CFC11 concentration is not significantly nonzero, so that the entire space below its matching line is allowed. $\Delta^{14}C$ rules out Γ greater than 240 years and less than 70 years. The combined CFC11-$\Delta^{14}C$ constraint permits a wide range of age spectra, as seen in the right panel. For example, delta function (pure advective) TTD are not ruled out. The true TTD is shown for comparison. For CCl_4-^{39}Ar the matching lines also intersect at (Γ, Δ) (160yrs, 80yrs). However, the CCl_4-^{39}Ar combined constraint including uncertainty is much more restrictive than CFC11-$\Delta^{14}C$, and the allowed age spectra cluster tightly around the true TTD.

[42] In this analysis we only exploit constraints on the age spectra provided by tracers. One could additionally use dynamical arguments to further constrain the TTD. For example, delta function age spectra in deep waters are not plausible dynamically, even if not strictly ruled out by available tracers. One expects that as the effects of mixing accumulate the TTD width should increase with distance along a dominant transport pathway from the surface. At the very least Δ should not decrease, because pure advection (bulk translation of the water mass and its properties) shifts the spectra to greater transit times but leaves the shape unchanged.

5.3. ΔDIC From Estimated Age Spectra

[43] The ranges of IG age spectra estimated by the tracers are now used to construct ranges for ΔDIC. The constraints the tracers impose on ΔDIC, via application of the age spectrum, are illustrated in Figure 7 for the cases of combinations CFC11-$\Delta^{14}C$ and CCl_4-^{39}Ar, each shown in model boxes 1, 3, and 9. Contour plots of ΔDIC from IG age spectra as a function of Γ and Δ are repeated for each box. In each case the dark shading indicates the intersection of the individual tracer constraints. The range of estimated ΔDIC from the two tracers in combination is the range of intersection of the ΔDIC contours with the dark shading. For box 1 CFC11 alone tightly constrains ΔDIC, despite the fact that the allowed (Γ, Δ) span a wide range. No additional constraint is provided by $\Delta^{14}C$. In this regime the CFC11 and ΔDIC contours are parallel, so that one acts as a good proxy for the other, regardless of the (Γ, Δ) used to construct either. Physically, being adjacent to the boundary layer, the water is dominated by young components, and is therefore nearly completely filled with CFC11 and recent ΔDIC. Over the narrow dominant TTD peak both CFC11 and ΔDIC vary approximately linearly and therefore similarly. Notice that in this box (but no other) τ_{CFC} τ_{DIC} (Figure 2), and the CFC11 lag method of ΔDIC works well (Figure 4).

[44] As progressively older locations are considered, the range of ΔDIC allowed by CFC11 alone becomes larger. For example, in box 5 CFC11 spans 11 to 30 pmole/kg of ΔDIC. Here, there are enough older water components that

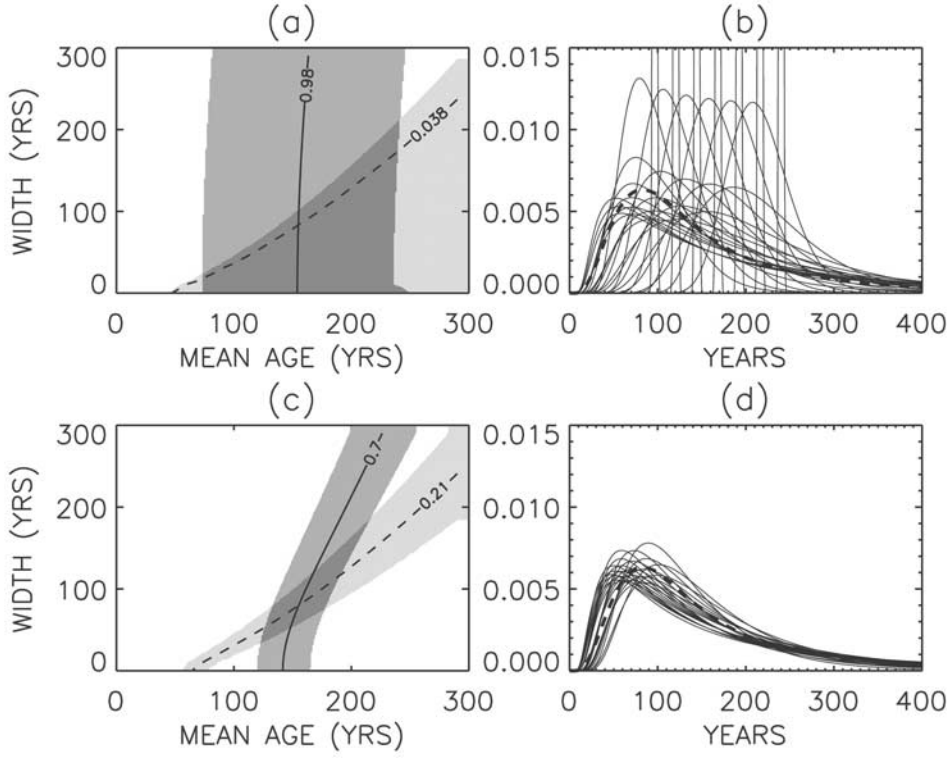

Figure 6. (a) Loci of (Γ, Δ) resulting in matches to box nine $\Delta^{14}C$ (solid line, labeled in fraction of surface layer concentration) and CFC11 (dashed line, labeled in pmole/kg). The light shaded (medium shaded) region indicates the allowed (Γ, Δ) from the CFC11 observational uncertainty ($\Delta^{14}C$ uncertainty). The dark shade is the intersection, the combined CFC11-$\Delta^{14}C$ constraint. (b) Sample TTDs corresponding to representative (Γ, Δ) pairs through the intersection region. The heavy dashed curve is the true TTD in box nine. (c, d) As in Figures 6a and 6b, respectively, but for ^{39}Ar (medium shade), CCL_4 (light shade) and the intersection (dark shade).

the surface history of CFC11 and ΔDIC look very different over the TTD. The $\Delta^{14}C$ constraint rules out large (Γ, Δ) allowed by CFC11, but these (Γ, Δ) correspond to little additional range in ΔDIC. Ruling out lower values of (Γ, Δ) would offer more leverage on ΔDIC, but the $\Delta^{14}C$ on box 5 is too uncertain to provide a lower bound. Thus, the CFC11 intersection with $\Delta^{14}C$ constitutes only a marginally tighter bound on ΔDIC (12 to 30 pmole/kg) than CFC11 alone. In box 9 CFC11 is not significantly different than zero, and delta function age spectra cannot be ruled out by CFC11 and $\Delta^{14}C$ (see Figure 6). Nonetheless, the addition of $\Delta^{14}C$ to CFC11 in box 9 offers more advantage for ΔDIC than it does in box 5. The delta function TTD at highest Γ permitted by $\Delta^{14}C$ still yield marginally nonzero ΔDIC estimates, because these Γ are all less than 250 years, the time ΔDIC has been present in surface waters. (A slower circulation, however, could have a CFC11–$\Delta^{14}C$ constraint allowing delta function TTD at Γ greater than 250 years, which would predict zero ΔDIC, even though the true ΔDIC could be nonzero; see section 5.4.) More importantly, box 9 $\Delta^{14}C$ rules out $\Gamma < 70$ years, which is permitted by CFC11 at small Δ, thereby prohibiting the ΔDIC > 16 μmol/kg allowed by CFC11.

[45] The combination CCl_4 and ^{39}Ar behave similarly, but the constraints on ΔDIC are tighter. Because the atmospheric history of CCl_4 is longer than CFC11, it exists in significant amounts in older waters. For this circulation, it is nonzero throughout the domain. Because ^{39}Ar decays more rapidly than $\Delta^{14}C$ its uncertainty covers a smaller range of Γ and Δ.

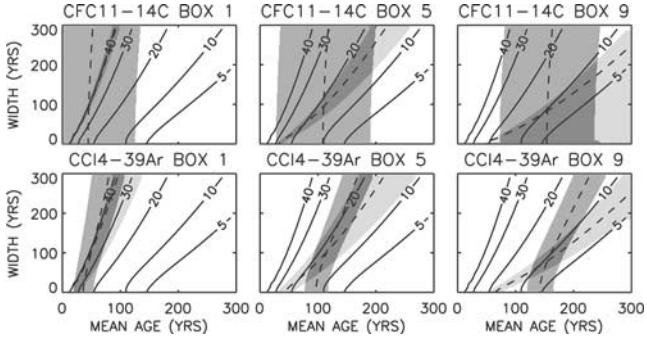

Figure 7. Contours of ΔDIC versus Γ and Δ (solid lines, labeled in μmole/kg), repeated for boxes 1, 5, and 9. Superposed on the top row are ranges allowed by CFC11 (light shade), $\Delta^{14}C$ (medium shade), and their intersection (dark shade), as well as the best estimate curves (dashed lines). On the bottom row are ranges allowed by CCl_4 (light shade), ^{39}Ar (medium shade), and their intersection (dark shade).

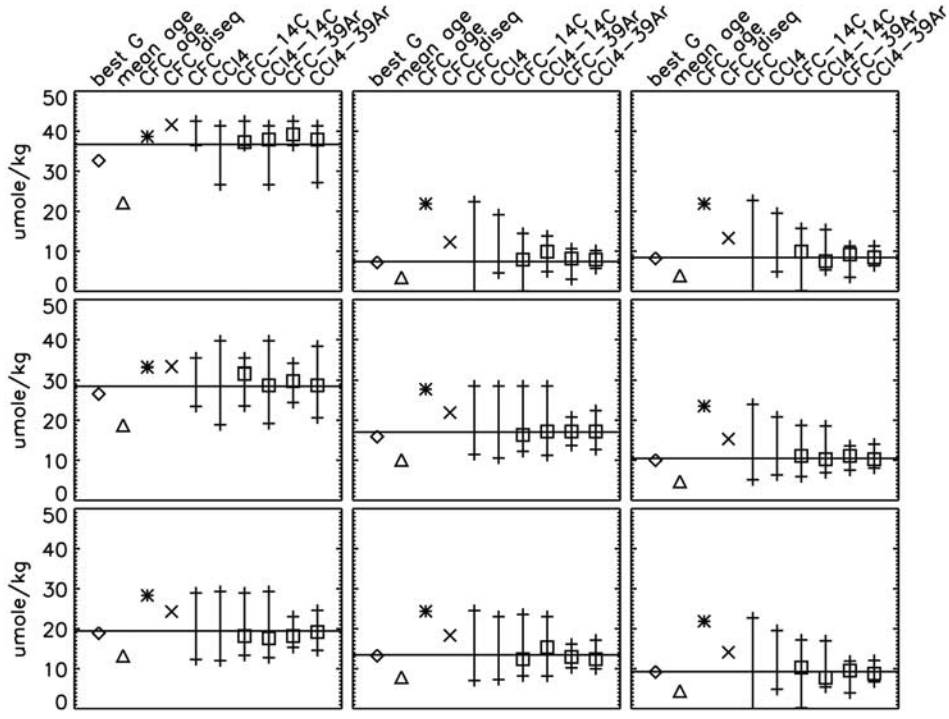

Figure 8. Estimated ΔDIC values from different methods for each model box. The first four estimates are repeated from Figure 4. The vertical bars correspond to ranges of ΔDIC estimated by the TTD method using various tracers singly or in combination, as labeled. For tracers in combination a best estimate can be calculated; its value is indicated by the square symbols. The horizontal line indicates the true ΔDIC.

[46] The ability of tracers to constrain ΔDIC throughout the domain is summarized in Figure 8, which shows ranges and best estimates of ΔDIC by the TTD technique using various tracers singly and in combination. When a single tracer is used (e.g., CFC11 or CCl_4 in Figure 8) only ranges result. There is no best estimate, because each tracer only limits (Γ, Δ) to a loci of values, even with no observational uncertainty. When the tracers are used in combination there is a best estimate, indicated by the symbol, and a range above and below due to observational uncertainty. The true ΔDIC, the value inferred from best-fit IG age spectra, the value inferred from Γ and τ_{CFC} lags, and that inferred employing the more restrictive use of τ_{CFC} by *Gruber et al.* [1996] are repeated from Figure 4 for comparison. Overall, the TTD method with any tracer or tracer combination performs better than using Γ or τ_{CFC} as a lag. The best estimates of ΔDIC from all the tracer combinations closely track the true ΔDIC, while the uncertainty ranges depend on the tracers. Even for CFC11 alone, the range of estimated ΔDIC brackets the true value, while the τ_{CFC} lag method is an overestimate. Note that the CFC11 concentration is insignificant in the oldest boxes (2, 3, and 9). It can therefore be used to put an upper bound on ΔDIC but no lower bound, a less biased use of CFC11 as a proxy for ΔDIC than lagging by τ_{CFC}.

[47] CCl_4 alone is a tighter constraint than CFC11 alone, and for this circulation is everywhere significantly nonzero. Thus CCl_4 everywhere places an upper and lower bound on ΔDIC. The combination of CFC11 and CCl_4 (not shown) is only marginally better than CCl_4 alone. The addition of $\Delta^{14}C$ to either CFC11 or CCl_4 narrows the ΔDIC range somewhat. For example, in box 2 $\Delta^{14}C$ reduces the upper ΔDIC bound provided by either CFC11 or CCl_4 alone. The addition of ^{39}Ar greatly reduces the ΔDIC range from either CFC11 or CCl_4. Adding further tracers to CCl_4-^{39}Ar or CFC11-^{39}Ar does not further reduce the ΔDIC range.

[48] The estimates of the total domain ΔDIC inventory are listed in Table 1 as a fraction of the "true" ΔDIC inventory. The τ_{CFC} lag method, at 1.63, is a large overestimate. (The uncertainty range on this ΔDIC estimate due to uncertainty in τ_{CFC} is small and does not encompass the true ΔDIC.) The Γ lag method, at 0.55, is a large underestimate. Using the transport component of the Gruber technique, which uses τ_{CFC} in a more restrictive fashion, results in 1.29, a more modest overestimate (see section 6). By contrast, all the TTD

Table 1. Total ΔDIC Inventories (Relative Units)

Method	ΔDIC
"True"	1.00
Best-fit 1-D TTD	0.94
Mean transit time lag	0.59
CFC11 age lag	1.60
CFC11 for disequilibrium term	1.29
CFC11 TTD constraint	0.65 to 1.54
CCl_4 TTD constraint	0.77 to 1.42
CFC11−$\Delta^{14}C$ TTD constraint	$1.03^{+0.13}_{0.16}$
CCl_4−$\Delta^{14}C$ TTD constraint	$1.01^{+0.13}_{0.17}$
CFC11−^{39}Ar TTD constraint	$1.03^{+0.09}_{0.07}$
CCl_4−^{39}Ar TTD constraint	$1.00^{+0.10}_{0.10}$

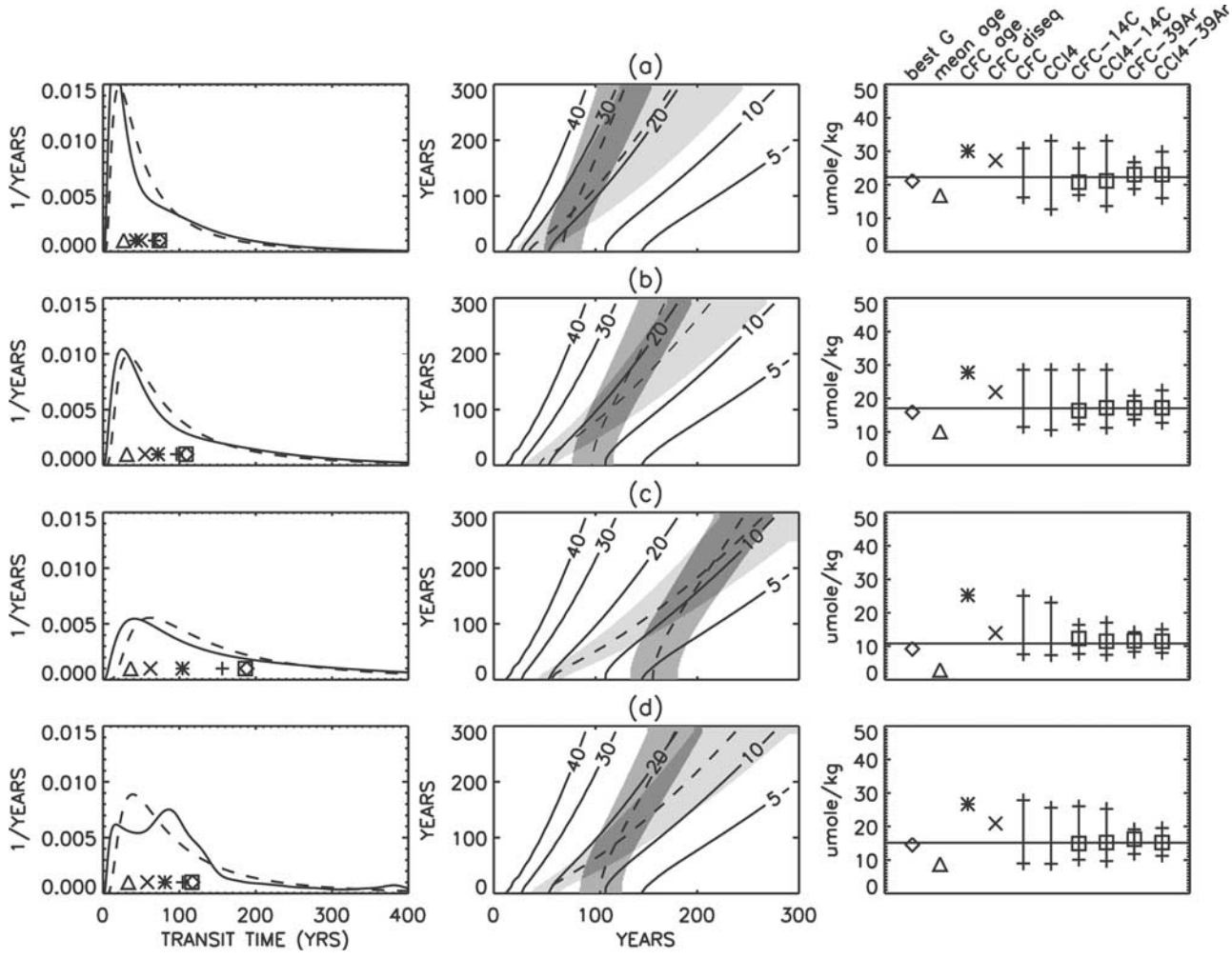

Figure 9. Box 5 TTD (left), allowed parameter ranges (center) and ΔDIC estimates (right) for four circulations. (a) "FAST" circulation, for which all advective fluxes are doubled compared to previous figures; (b) "MEDIUM" circulation, identical to previous figures; (c) "SLOW" circulation, for which all advective fluxes are halved; (d) circulation with "CYCLES," for which the advective fluxes connecting the upper six boxes vary sinusoidally with six frequency components ranging from $2\pi/350$ years ^{1} to $2\pi/50$ years ^{1}, all having amplitude 0.25 times the steady MEDIUM circulation fluxes and randomly selected phases.

methods give constraints bracketing the true value. The use of CFC11 alone gives an upper bound of 1.54, close to the τ_{CFC} method, but has a lower bound (0.65) well below the "true" value. The TTD technique thus uses CFC11 in a less biased way. When tracer combinations are considered the inventory constraints are tighter. The combination CFC11-Δ^{14}C gives $1.03^{+0.13}_{0.16}$. CFC11-^{39}Ar, the tightest constraining pair, gives $1.03^{+0.09}_{0.07}$. Note that domain summing can result in canceling errors. For example, on a domain scale CCl_4 alone is more accurate than CFC11 alone, because it is everywhere nonzero. However, in young regions CFC11 is more accurate, because it has a smaller uncertainty.

5.4. Sensitivity to Circulation

[49] In order to check that the apparent merit of the TTD approach is not just a consequence of the particular circulation selected for our simple model (termed "MEDIUM"), we repeat the analysis for a circulation in which advective fluxes are everywhere halved ("SLOW") and everywhere doubled ("FAST"). We also test a circulation ("CYCLES") for which the advective fluxes connecting the upper six boxes vary sinusoidally with six frequency components ranging from $2\pi/350$ years ^{1} to $2\pi/50$ years ^{1}, all having amplitude 0.25 times the steady MEDIUM circulation fluxes and randomly selected phases. The results on box 5 are shown in Figure 9. Increasing the circulation results in younger water, higher ΔDIC and higher estimates of ΔDIC for all techniques. Decreasing the circulation results in older water, lower ΔDIC and lower ΔDIC estimates. The relative performance of the techniques is little changed, however. Periodic variations in the circulation cause "wiggles" in the TTD, but have little impact on the accuracy of the ΔDIC inferences.

[50] Age spectra in the real ocean could be very different than the age spectra for any of the circulations of our simple model. Two points can be made, however: (1) As noted previously, the simple model's age spectra are similar in overall shape to those seen in several GCM studies [*Khatiwala et al.*, 2001; *Thomas et al.*, 2001; *Haine and Hall*, 2002]. (2) Differences among observed tracer ages indicate that age spectra in the real ocean must have significant width; that is, they cannot be the delta functions of pure bulk advection. In the deep ocean this is illustrated by the typical 50% differences between ^{39}Ar and Δ^{14}C ages [*Broecker and Peng* [2000]. For younger water *Waugh et al.* [2002] argue that differences in CFC and ^{3}H/^{3}He ages, noted by *Doney et al.* [1997], are consistent with TTD widths that are a large fraction of the mean transit time. Thus, even if real ocean age spectra are different than the age spectra of our simple model or the IG form, these observations suggest that the estimation of two temporal moments (mean and width) is an important step beyond using single tracer ages as lags for ΔDIC, which implicitly assumes delta function age spectra.

6. Comparison to Technique of *Gruber et al.* [1996]

[51] *Gruber et al.* [1996] developed and applied a technique (hereafter called the Gruber technique) to infer ΔDIC from measurements of total DIC. Their technique, applied in several subsequent analyses [*Gruber*, 1998; *Sabine et al.*, 1999] represents an important advance in quantifying anthropogenic carbon in the ocean. Several recent studies have compared the Gruber technique to other techniques [e.g., *Coatanoan et al.*, 2001; *Sabine and Feely*, 2001]. Here, we are address the limits of the representation of transport in the Gruber technique. We begin with a brief review.

[52] *Gruber et al.* [1996] construct a quasiconserved tracer C* by adding other constituents to total DIC that compensate for carbon conversions due to natural biogeochemical processes; i.e., the "soft-tissue pump" and "carbonate pump." At the sea surface C* = DIC. As water penetrates the interior, carbon cycles among its biochemical reservoirs, but C* is approximately conserved. The anthropogenic component is $\Delta DIC = C^*_{obs} - C^*_{pre}$, where C^*_{obs} is the total observed concentration and C^*_{pre} is the preindustrial concentration. Unfortunately, C^*_{pre} is not directly known. *Gruber et al.* [1996] express it for each outcrop of an isopycnal surface as $C^*_{pre} = C^*_{eq,\,pre} - C^*_{diseq}$, where $C^*_{eq,\,pre}$ is the concentration in saturated equilibrium with the preindustrial atmosphere for the outcrop (determined by solving the equilibrium carbonate system given knowledge of preindustrial atmospheric CO_2) and C^*_{diseq} (the "disequilibrium term") is the degree to which the ocean circulation prevents air-sea equilibrium from being achieved at the outcrop. The Gruber technique estimates C^*_{diseq} in two different ways, depending on the isopycnal surface under consideration. If somewhere on the surface there is water old enough to be uncontaminated by anthropogenic carbon, then $C^*_{diseq} = C^*_{eq,\,pre} - C^*_{obs}$(old), where C^*_{obs}(old) is the observed concentration in these old waters. In other words, $C^*_{pre} = C^*_{obs}$(old). In the *Gruber* [1998] Atlantic Ocean analysis, C^*_{diseq} for these deep isopycnal surfaces is computed for two outcrops, in high northern and southern latitudes, using PO_4^* as a discriminator of surface origin [*Broecker et al.*, 1991]. An average C^*_{diseq} weighted by the relative outcrop contributions is then applied to all water on the isopycnal surface, including contaminated water.

[53] For more rapidly ventilated isopycnal surfaces no such uncontaminated water exists to determine C^*_{diseq}. By the Gruber technique one obtains C^*_{diseq} for these surfaces in the following manner: Tracer "ages" τ (e.g., τ_{CFC}) are used to estimate the date that a water mass was last at the surface. The saturated equilibrium C^*_{eq} appropriate for atmospheric CO_2 levels at this past date, $C^*_{eq}(t - \tau)$, is computed from knowledge of atmospheric CO_2, and $C^*_{diseq} = C^*_{eq}(t - \tau) - C^*_{obs}$. Upon substitution, one then has

$$\Delta DIC = C^*_{eq}(t - \tau) - C^*_{eq,pre} \qquad (3)$$

which is the statement of the approximation (shown to be poor in our analysis) that interior ΔDIC can be determined from the ΔDIC surface time series with a single age, for example τ_{CFC}. Expression (3) amounts to applying a $\delta(t - \tau)$ TTD to the BC $C^*_{eq}(t) - C^*_{eq,\,pre}$, which is the same BC we use. Our approach generalizes (3) by allowing a more realistic TTD; that is, by applying expression (1) to the BC we have, instead of (3),

$$\Delta DIC(r,t) = \int_0^\infty C^*_{eq}(t - \xi)\mathcal{G}(r,\xi)d\xi - C^*_{eq,pre} \qquad (4)$$

Recognizing the potential for error *Gruber et al.* [1996] and *Gruber* [1998] do not use (3) directly. Instead, *Gruber* [1998] calculates C^*_{diseq}, using CFC11 on each outcrop only for waters with $\tau_{CFC} - 30$ years and water mass contribution from the outcrop greater than 80%. Averaging the resulting C^*_{diseq} estimates provides an effective C^*_{diseq} for the isopycnal surface.

[54] If this analysis over/underestimates C^*_{diseq} then it over/underestimates ΔDIC by an equal amount. Shown in Figures 4 and 8 are ΔDIC estimates of the Gruber C^*_{diseq} approach applied to our simple model (called "CFC diseq" in the figure). In this application of the model we consider it to represent a single isopycnal surface that has one outcrop and that is "fully contaminated" with ΔDIC. We obtained the Gruber ΔDIC by adding to the "true" ΔDIC (the value simulated directly in the model) the Gruber error in C^*_{diseq}, which is just the difference in the ΔDIC BC evaluated at $t - \tau_{CFC}$ and $t - \tau_{DIC}$ (t is the present time) averaged over all model boxes having $\tau_{CFC} - 30$ years. (The value τ_{DIC}, not known in advance, would be the only correct single "age" to use for C^*_{diseq}, as it is by definition the elapsed time since the surface displayed the C* of the water mass.) Everywhere $\tau_{CFC} < \tau_{DIC}$, as seen in Figure 2. Thus, when comparing the surface $C^*_{eq}(t)$ to C^*_{obs} to get C^*_{diseq}, one does not look far enough back in time. The C^*_{diseq} and ΔDIC are therefore overestimated, in this case by 4.9 μmole/kg. Note that this error is caused solely by the representation of transport in the Gruber technique. No analysis of the representation of carbon biochemistry is made here; that is, the construction of the conservative tracer C* is assumed to be perfect.

[55] The 4.9 μmole/kg overestimate is a significantly smaller error than using τ_{CFC} as a lag time throughout the hypothetical isopycnal surface, as is seen in Figures 4 and 8. The error in the Gruber analysis is smaller because it arises from biases in τ_{CFC} only over the young regions of the isopycnal surface where τ_{CFC} 30 years (boxes 1, 4, and 7). In these regions CFCs are better proxies of ΔDIC than in older regions. However, because the resulting C^*_{diseq} estimate applies over the whole isopycnal surface, its error is a large fraction of the smaller ΔDIC levels of older regions (boxes 2, 3, 4, and 5 in Figures 4 and 8). *Gruber* [1998] quotes a ΔDIC uncertainty due to τ_{CFC} of 3 μmole/kg, based on the observation that ages derived from CFC11 and $^3H/^3He$ are within eight years of each other for τ_{CFC} 30 years [*Doney et al.*, 1997]. However, for ΔDIC estimation the more relevant comparison is between τ_{CFC} and τ_{DIC}, which differ by 20 years for τ_{CFC} = 30 years in our simple model, by 30 to 60 years in an analysis of ΔDIC inference techniques by *Coatanoan et al.* [2001], and even more for some combinations of advection and diffusion in the study of *Waugh et al.* [2002]. Moreover, the error in C^*_{diseq} (and therefore ΔDIC) from use of τ_{CFC} is systematic, so that it accumulates in domain inventories. The inventory over the hypothetical isopycnal surface represented by our simple model is overestimated by 29% using the Gruber C^*_{diseq} technique (Table 1). (Other circulations for the model yield different fractional errors.)

[56] Errors in the ΔDIC inventory of deep isopycnal surfaces could also arise if regions that were believed to be uncontaminated instead had small but nonzero ΔDIC. Application of the Gruber technique to such an isopycnal surface would result in an underestimate of ΔDIC over the whole surface, as C^*_{diseq} would be underestimated (C^*_{pre} overestimated). As *Gruber* [1998] notes, a 2 μmol/kg systematic error in deep North Atlantic C^*_{dis} leads to an approximate 20% error in total water column inventory. The possibility of this systematic error, in fact, largely determines the inventory uncertainties quoted by *Gruber* [1998]. Are 2 μmol/kg ΔDIC concentrations in the deep Atlantic plausible? *Broecker and Peng* [2000] analyze $\Delta^{14}C$ and ^{39}Ar observations in Atlantic regions deep enough that they would be treated as uncontaminated in the Gruber analysis. For example, at 18 N, 54 W and 2.8 km depth *Broecker and Peng* [2000] report $\Delta^{14}C$ = 0.97 and ^{39}Ar = 0.57 (stated as fractions of North Atlantic surface water concentrations), giving τ_{14C} = 252 years and τ_{39Ar} = 219 years. Neglecting observational uncertainties for the moment, these data constrain the IG TTD form to Γ = 254 years and Δ = 136 years. Convolving this IG TTD with the ΔDIC surface BC yields ΔDIC = 4.5 μmol/kg.

[57] Now, the 4.5 μmol/kg value is not likely to be accurate, nor have we even demonstrated it to be statistically different than zero. There is considerable uncertainty on τ_{14C} and τ_{39Ar}. In addition, the IG TTD form works poorly when applied to a tracer that, because of its short history, is only sensitive to the leading fraction of the TTD, as is the case for ΔDIC in these old waters. An erroneous shape of the leading edge of the TTD may cause only relatively small errors in Γ and Δ, but the effect on the tracer is greatly magnified. Finally, we are neglecting contributions to the water mass from southern hemisphere sources. Nonetheless, the magnitude of this ΔDIC estimate from τ_{14C} and τ_{39Ar} suggests that 2 μmole/kg errors in C^*_{diseq} for the deep Atlantic cannot be ruled out and raises the possibility of significant inventory errors. The key feature is that τ_{14C} is significantly larger than τ_{39Ar} throughout the deep Atlantic [*Broecker and Peng*, 2000], implying broadly distributed TTDs. This is true even if the details of the TTD do not match the IG form. Therefore, even though Γ may be greater than 250 years (the history of ΔDIC in surface waters) there is still a significant fraction of water with transit time less than 250 years, and this fraction contains nonzero ΔDIC.

[58] It is important to note that, assuming other uncertainties to be neutral, the neglect of mixing in the Gruber technique leads to overestimates of ΔDIC on fully contaminated isopycnal surfaces and underestimates on "uncontaminated" surfaces. These errors will tend to cancel in domain-wide inventories. In addition, we have only addressed the representation of transport in the Gruber technique. Biogeochemical issues related to the compensation of natural sources and sinks by the inclusion of additional constituents are beyond the scope of this study. Finally, we note that the TTD could be used in the context of the Gruber technique. Instead of $C^*_{diseq} = C^*_{eq}(t \quad \tau)$ C^*_{obs} one could compute

$$C^*_{diseq} = \int_0^\infty C^*_{eq}(t \quad t')\mathcal{G}(r,t')dt' \quad C^*_{obs}(r,t) \qquad (5)$$

where the TTD $\mathcal{G}$ is estimated as best as possible from available tracers. Compared to using the TTD directly (5) has the advantage of not requiring tracer observations over the entire isopycnal surface under analysis, although C* measurements are required. The TTD need only be estimated over a limited region to determine C^*_{diseq}, which is then applied to the entire surface. The use of $\mathcal{G}$, even constrained solely by CFCs, would be an improvement over the τ_{CFC} approach. The TTD-estimated C^*_{diseq} would have comparable uncertainty but would be less biased.

7. Summary and Discussion

[59] We have described a technique (the "transit time distribution," or TTD, technique) for estimating concentrations of anthropogenic carbon from observable tracers, and have illustrated the technique with an idealized model. Unlike techniques that rely on single tracer ages, which effectively assume the transport to be purely bulk advective, the TTD technique naturally includes the effects of mixing. Following *Thomas et al.* [2001], transport from the surface to interior points is represented by distributions of transit times (age spectra). However, while *Thomas et al.* [2001] use GCMs to generate TTDs, we describe a way to estimate TTDs directly from tracer observations. We use tracers in combination to constrain two temporal moments of a TTD, equivalent to the mean ventilation time and the spread of ventilation times. From inception the TTD technique considers only the anthropogenic carbon component ΔDIC. The tracer-estimated TTDs propagate into the inte-

rior a time series of ΔDIC in surface waters, which is constructed from marine carbonate system analysis. Thus, no separation of the small anthropogenic component from the large and variable natural ocean carbon cycle is required.

[60] In a comparison using synthetic data from a simple model the TTD technique provides a more accurate estimate of ΔDIC and a more natural assessment of uncertainty than several other approaches. Using CFC age to propagate the surface ΔDIC evolution into the interior results in a large overestimate of ΔDIC through much of the domain. A smaller but still significant overestimate results from limiting the use of CFC to water having τ_{CFC} 30 years, as is done for ''fully contaminated'' isopycnal surfaces by *Gruber* [1998]. Because of mixing, a range of ages is present in any water mass. CFCs only provide information about components that are younger than 50 years, while anthropogenic carbon is present in components up to 250 years. In the TTD technique the effects of mixing are included implicitly, because continuous distributions of ages are considered. In addition, the technique provides a natural translation of the uncertainties in individual tracers to an uncertainty in inferred ΔDIC. In contrast to approaches using a single tracer age, the uncertainty in ΔDIC inferred by the TTD technique bounds the true ΔDIC.

[61] The tightest ΔDIC constraint in the TTD technique is provided by using two tracers in combination. The tracers should be significantly different in their temporal variation (for transient tracers) or radioactive decay (for natural radioisotopes), and at least one should have a timescale comparable to or greater than the history of anthropogenic carbon (250 years). CFCs or CCl_4 or $^3H/^3He$ in combination with ^{39}Ar or natural $\Delta^{14}C$ are possible combinations, although $\Delta^{14}C$ is limited by uncertainty in the surface water BC for these timescales, which are short compared to $\Delta^{14}C$ decay. The combination of ^{39}Ar with either a CFC or CCl_4 provides tight upper and lower bounds on ΔDIC. Unfortunately, ^{39}Ar is expensive to measure, and there are only the order of 100 measurements globally. However, the TTD approach has benefits even using a CFC alone as a constraint. The resulting ΔDIC estimates have uncertainty comparable to using CFC age as a lag time, but they are less biased. In fact, using only CFCs the TTD approach could be applied in the context of the *Gruber et al.* [1996] technique to provide less biased estimates of C^*_{diseq}, the air-sea ''disequilibrium'' term.

[62] This study demonstrates promise for the TTD approach to ΔDIC estimation. Important testing remains to be done, however. We have considered only one surface source region for tracers in our analysis. We plan to repeat the analysis with three-dimensional numerical models to generate more realistic TTDs, having multiple source regions. Among other things, this will allow us to test more thoroughly the applicability of the IG TTD form. More generally, it would be valuable to perform systematic comparisons and evaluations of various ΔDIC inference techniques in the context of an ocean GCM with carbon biochemistry, where the true answer is known. Such testing will allow the relative advantages and disadvantages of different ΔDIC inference techniques be assessed in detail.

[63] **Acknowledgments.** We thank the ''age group'' at the Lamont-Doherty Earth Observatory for lively discussions and Mick Follows and Helmuth Thomas for assistance with the equilibrium carbonate system. Comments from an anonymous reviewer led to an improved manuscript. This work was supported in part by a grant from the Physical Oceanography Program of the National Science Foundation (OCE-9911598).

References

Beining, P., and W. Roether, Temporal evolution of CFC11 and CFC–12 concentrations in the ocean interior, *J. Geophys. Res.*, *101*, 16,455–16,464, 1996.

Broecker, W. S., and T.-H. Peng, Comparison of ^{39}Ar and $\Delta^{14}C$ ages for waters in the deep ocean, *Nucl. Instrum. Methods Phys. Res., Sect. B*, *172*, 473–478, 2000.

Broecker, W. S., et al., Preliminary estimates for the radiocarbon age of deep water in the glacial ocean, *Paleoceanography*, *3*, 659–669, 1988.

Broecker, W. S., et al., Radiocarbon decay and oxygen utilization in the deep Atlantic Ocean, *Global Biogeochem. Cycles*, *5*, 87–117, 1991.

Broecker, W. S., et al., Oceanic radiocarbon: Separation of the natural and bomb components, *Global Biogeochem. Cycles*, *9*, 263–288, 1995.

Coatanoan, C., et al., Comparison of two approaches to quantify anthropogenic CO_2 in the ocean: Results from the northern Indian Ocean, *Global Biogeochem. Cycles*, *15*, 11–25, 2001.

Deleersnijder, E., et al., The concept of age in marine modelling, 1, Theory and preliminary model results, *J. Mar. Syst.*, *28*, 229–267, 2001.

Delhez, E., et al., Toward a general theory of age in ocean modelling, *Ocean Modell.*, *1*, pp. 17–27, Hooke Inst. Oxford Univ., Oxford, England, 1999.

Dickson, A. G., and F. J. Millero, A comparison of the equilibrium constants for the dissociation of carbonic acid in seawater media, *Deep Sea Res.*, *34*, 1733–1743, 1987.

Doney, S. C., et al., A comparison of ocean tracer dating techniques on a meridional section in the eastern North Atlantic, *Deep Sea Res., Part 1*, *44*, 603–626, 1997.

England, M. H., and E. Maier-Reimer, Using chemical tracers to assess ocean models, *Rev. Geophys.*, *39*, 29–70, 2001.

Fiadiero, M. E., Three-dimensional modeling of tracers in the deep Pacific Ocean, 2, Radiocarbon and the circulation, *J. Mar. Res.*, *40*, 537–550, 1982.

Goyet, C., and P. G. Poissonn, New determination of carbonic acid dissociation constants in seawater as a function of temperature and salinity, *Deep Sea Res.*, *36*, 2635–2654, 1989.

Goyet, C., et al., Spatial variation of total CO_2 and total alkalinity in the northern Indian Ocean: A novel approach for the quantification of anthropogenic CO_2 in seawater, *J. Mar. Res.*, *57*, 135–163, 1999.

Gruber, N., Anthropogenic CO_2 in the Atlantic Ocean, *Global Biogeochem. Cycles*, *12*, 165–191, 1998.

Gruber, N., J. L. Sarmiento, and T. F. Stocker, An improved method for detecting anthropogenic CO_2 in the oceans, *Global Biogeochem. Cycles*, *10*, 809–837, 1996.

Haine, T. W. N., and T. M. Hall, A generalized transport theory: Water mass composition and age, *J. Phys. Oceanogr.*, *32*, 1932–1946, 2002.

Haine, T. W. N., et al., The flow of Antarctic bottom water to the southwest Indian Ocean estimated using CFCs, *J. Geophys. Res.*, *103*, 27,637–27,653, 1998.

Hall, T. M., and R. A. Plumb, Age as a diagnostic of stratospheric transport, *J. Geophys. Res.*, *99*, 1059–1070, 1994.

Hall, T. M., et al., Evaluation of transport in stratospheric models, *J. Geophys. Res.*, *104*, 18,815–18,839, 1999.

Holzer, M., and T. M. Hall, Transit-time and tracer-age distributions in geophysical flows, *J. Atmos. Sci.*, *57*, 3539–3558, 2000.

Huhn, O., W. Roether, P. Beining, and H. Rose, Validity limits of carbon tetrachloride as an ocean tracer, *Deep Sea Res., Part I*, *48*, 2025–2049, 2001.

Hunter-Smith, R. J., et al., Henry's law constants and the air-sea exchange of various low molecular weight halocarbon gases, *Tellus, Ser. B*, *35*, 170–176, 1983.

Jenkins, W. J., ^3H and ^4He in the Beta Triangle: Observations of gyre ventilation and oxygen utilization rates, *J. Phys. Oceaogr.*, *17*, 763–783, 1987.

Johnson, D. G., et al., Stratospheric age spectra derived from observations of water vapor and methane, *J. Geophys. Res.*, *104*, 21,595–21,602, 1999.

Khatiwala, S., M. Visbeck, and P. Schlosser, Age tracers in an ocean GCM, *Deep Sea Res., Part A*, *48*, 1423–1441, 2001.

Lewis, E. and D. W. R. Wallace, Program developed for CO_2 system calculations, *ORNL/CDIAC-105*, Carbon Dioxide Inf. Anal. Cent., Oak Ridge Natl. Lab., U. S. Dep. of Energy, Oak Ridge, Tenn, 1988.

Maier-Reimer, E., et al., Future ocean uptake of CO_2: Interaction between ocean circulation and biology, *Clim. Dyn.*, *12*, 711–721, 1996.

Mehrbach, C., C. H. Culberson, J. E. Hawley, and R. M. Pytkowicz, Measurement of the apparent dissociation constants of carbonic acid in seawater at atmospheric pressure, *Limnol. Oceanogr.*, *18*, 897–907, 1973.

Meredith, M. R., et al., On the use of carbon tetrachloride as a transient tracer of Weddell Sea deep and bottom waters, *Geophys. Res. Lett.*, *23*, 2943–2946, 1996.

Millero, F. J., P. Roche, and K. Lee, The total alkalinity of Atlantic and Pacific waters, *J. Mar. Chem.*, *60*, 111–130, 1998.

Plattner, G.-K., et al., Feedback mechanisms and sensitivities of ocean carbon uptake under global warming, *Tellus, Ser. B*, *53*, 564–592, 2001.

Roy, R. N., et al., The dissociation constants of carbonic acid in seawater at salinities 5 to 45 and temperatures 0 to 45 deg C, *J. Mar. Chem.*, *44*, 249–267, 1993.

Sabine, C. L., and R. A. Feeley, Comparison of recent Indian Ocean anthropogenic CO_2 estimates with a historical approach, *Global Biogeochem. Cycles*, *15*, 33–42, 2001.

Sabine, C. L., et al., Anthropogenic CO_2 inventories in the Indian Ocean, *Global Biogeochem. Cycles*, *13*, 179–198, 1999.

Sarmiento, J. L., and S. C. Wofsy, A U. S. carbon cycle science plan: Report of the Carbon and Climate Working Group, report, U. S. Global Change Res. Program, Washington, D. C., 2000.

Schlitzer, R., et al., A meridional ^{14}C and ^{39}Ar section in Northeast Atlantic Deep Water, *J. Geophys. Res.*, *90*, 6945–6952, 1985.

Seshadri, V., *The Inverse Gaussian Distribution: Statistical Theory and Applications*, Springer-Verlag, New York, 1999.

Thiele, G., and J. L. Sarmiento, Tracer dating and ocean ventilation, *J. Geophys. Res.*, *95*, 9377–9391, 1990.

Thomas, H., and V. Ittekkot, Determination of anthropogenic CO_2 in the North Atlantic Ocean using water mass age and CO_2 equilibrium chemistry, *J. Mar. Syst.*, *27*, 325–336, 2001.

Thomas, H., M. H. England, and V. Ittekkot, An off-line 3D model of anthropogenic CO_2 uptake by the oceans, *Geophys. Res. Lett*, *28*, 547–550, 2001.

Walker, S. J., et al., Reconstructed histories of the annual mean atmospheric mole fractions for the halocarbons CFC11, CFC–12, CFC113 and carbon tetrachloride, *J. Geophys. Res.*, *105*, 14,285–14,296, 2000.

Wallace, W. R. D., Introduction to special section: Ocean measurements and models of carbon sources and sinks, *Global Biogeochem. Cycles*, *15*, 3–10, 2001.

Wallace, W. R. D., et al., Carbon tetrachloride and chlorofluorocarbons in the South Atlantic Ocean, 19 S, *J. Geophys. Res.*, *99*, 7803–7819, 1994.

Wanninkhof, R., S. C. Doney, T.-H. Peng, J. L. Bullister, K. Lee, and R. A. Feely, Comparison of methods to determine the anthropogenic CO_2 invasion into the Atlantic Ocean, *Tellus, Ser. B*, *51*, 511–530, 1999.

Warner, M. J., and R. F. Weiss, Solubilities of chlorofluorocarbons 11 and 12 in water and sea water, *Deep Sea Res., Part A*, *32*, 1485–1497, 1985.

Waugh, D. W., and T. M. Hall, Age of stratospheric air: Theory, observations, and models, *Rev. Geophys.*, doi:10.1029/2000RG000101, in press, 2002.

Waugh, D. W., T. M. Hall, and T. W. N. Haine, Relationships among tracer ages, *J. Geophys. Res.*, doi:10.1029/2002JC001325, (in press), 2002.

T. M. Hall, NASA Goddard Institute for Space Studies, 2880 Broadway, New York, NY 10025, USA. (thall@giss.nasa.gov)

T. W. N. Haine and D. W. Waugh, Department of Earth and Planetary Sciences, Johns Hopkins University, Baltimore, MD 21218, USA. (Thomas.Haine@jhu.edu; waugh@jhu.edu)